Study of Localized Solutions of the Nonlinear Discrete Model for Dipolar BEC in an Optical Lattice by the Homoclinic Orbit Method

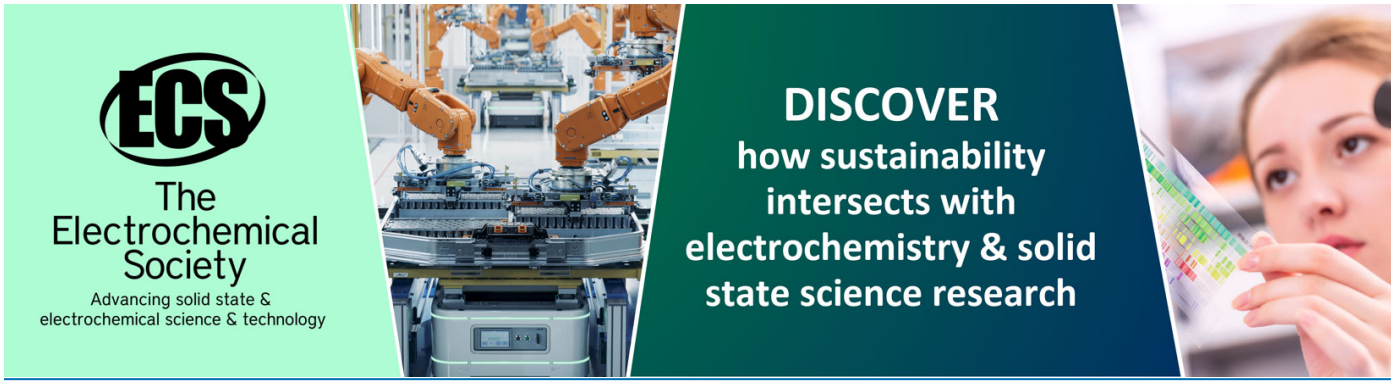

Journal of Physics: Conference Series **435** (2013) 012026 doi:10.1088/1742-6596/435/1/012026

Study of Localized Solutions of the Nonlinear Discrete Model for Dipolar BEC in an Optical Lattice by the Homoclinic Orbit Method

Azeddine Messikh[1] **and Bakhram Umarov**[2]

[1] Kulliyah of Information and Communication Technology, IIUM, Jalan Gombak 53100, Kuala Lumpur, Malaysia.

[2] Kulliyyah of Science, IIUM, Jalan Sultan Ahmad Shah, Bandar Indera Mahkota, 25200 Kuantan, Pahang, Malaysia.

E-mail: messikh@iium.edu.my

Abstract. We use homoclinic orbits to find solutions of a dynamical system of the dipolar Bose Einstein Condensate (BEC) in a deep optical lattice. The equation of motion is transformed to a two-dimensional map and its homoclinic orbits are computed numerically. Each homoclinic orbit leads to a different solution. These different solutions lead to different types of solitons. We also analyse the stability of the solutions.

1. Introduction

It is well known that the dynamics of the Bose Einstein condensate (BEC) trapped in an optical lattice can be described in tight-binding approximation by the discrete Nonlinear Schrödinger Equation (DNLSE) [1, 2]. This model opens the way to study different aspects of the BEC dynamics in an optical lattice, such as discrete solitons and nonlinear localized modes and their stability and dynamics, modulational instability, superfluid-insulator transition, etc. [3]. Also recently the nonlinearity caused by long range dipole-dipole interaction attracts much interest [4,5]. In this case the corresponding discrete model for dipolar BEC in an optical lattice was introduced in the work [6], and further investigated in [7].

The equation for one dimensional optical lattice in the dimensionless variables was derived in [8] and the nonlinear localized modes has been investigated in details by application of numerical Newton-Raphson method. In this work, following the paper [9] we rather use homoclinic orbits to find the localized solutions. The equation of motion is transformed to a two-dimensional map and the homoclinic orbits for this map are computed numerically. Each homoclinic orbit leads to a different solution. Also the linear stability of the found solutions is investigated.

2. Two-Dimensional map

Consider the dipolar Bose Einstein Condensate (BEC) in a deep optical lattice. It is well known that the governing equation for this system is given by [6–8]

$$i\frac{d}{dt}\Phi_n + \kappa(\Phi_{n+1} + \Phi_{n-1}) + q|\Phi_n|^2\Phi_n + g\left(|\Phi_{n+1}|^2 + |\Phi_{n-1}|^2\right)\Phi_n = 0, \tag{1}$$

where Φ_n is the complex field amplitude at the n-th site of the lattice, and κ is the linear parameter, while q and g correspond to the nolinearity parameters. This equation, which is 1D equation, has no exact analytical solution. Therefore, we use numerical methods and look for localized stationary solutions of the form

$$\Phi_n = u_n e^{i\omega t}. \tag{2}$$

If we substituted this form into the equation of motion (1), we get

$$q\,u_n^3 + \left[g\,\left(u_{n+1}^2 + u_{n-1}^2\right) - \omega\right]\,u_n + \left(u_{n+1} + u_{n-1}\right)\kappa = 0. \tag{3}$$

It easy to show that this last equation has at most three fixed points

$$p_0 = 0 \text{ and } p_\pm = \pm\sqrt{\frac{\omega - 2\kappa}{2g+q}}. \tag{4}$$

It is worth mentioning that $p_\pm$ should be real numbers.

With the transformation $v_n = u_{n-1}$, Eq. (3) becomes a two-dimensional map

$$\begin{cases} u_{n+1} &= 2\dfrac{(\omega - gv_n^2)u_n - qu_n^3 - \kappa v_n}{\kappa \pm \sqrt{\kappa^2 + 4g(\omega - gv_n^2)u_n^2 - 4gqu_n^4 - 4g\kappa u_n v_n}}, \\ v_{n+1} &= u_n. \end{cases} \tag{5}$$

In what follows we restrict to the case when $\kappa > 0$ and to the map that corresponds to the denominator $\kappa + \sqrt{\kappa^2 + 4g(\omega - gv_n^2)u_n^2 - 4gqu_n^4 - 4g\kappa u_n v_n}$. Since u_n and v_n are real numbers, the map exists only when

$$\kappa^2 + 4g(\omega - gv_n^2)u_n^2 - 4g(qu_n^3 + \kappa v_n)u_n \geq 0. \tag{6}$$

Some examples for the existence of the map are shown by the dashed area in Fig. 1.

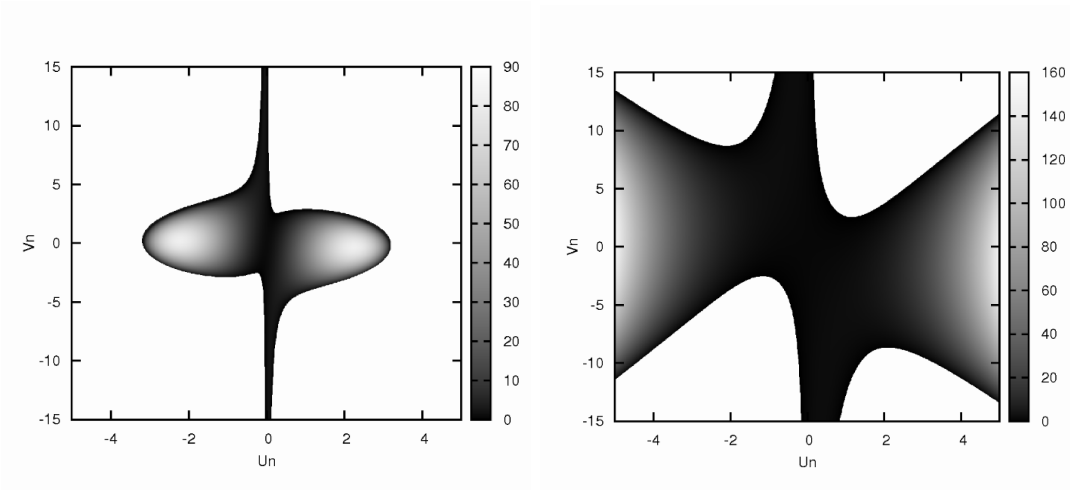

Figure 1. The map exists only in the dashed area. The parameters used are: (left figure) $\kappa = 1$, $q = 1$, $g = 0.8$, $\omega = 10$ and (right figure) $\kappa = 1$, $q = -0.6$, $g = 0.1$ and $\omega = 0.1$. These homoclinic points lead to three different solitons.

To get some solutions of Eq. (1), we fellow the method described in [10] which is based on homoclinic orbits. This method is briefly reviewed in the next section.

3. Homoclinic orbits

There are two interesting manifolds for a two-dimensional map, stable manifold and unstable manifold. The stable (unstable) manifold is the set of points that converge to a saddle fixed point through forward (backward) iterations of the map. It is well know that a fixed point in two-dimensional map is a saddle point if the two eigenvalues of its Jacobian, $\lambda_{\pm}$, satisfy the following inequalities

$$|\lambda_-| < 1 \quad \text{and} \quad |\lambda_+| > 1. \tag{7}$$

The stable manifold corresponds to the eigenvalue λ_-, while the unstable manifold corresponds to the other eigenvalue λ_+. An intersection point of the stable and unstable manifolds is called a homoclinic point. The orbit that contains this point is called a homoclinic orbit. It is clear that any point in a homoclinic orbit will converge to the saddle fixed point by forward and backward iterations. Therefore, homoclinic orbits give stationary solutions for Eq. (1) with the form given by Eq. (2) and converges to corresponding saddle fixed point.

Returning back to our map, Eq.(5). At the fixed point p_0 , the Jacobian matrix of the map for $\kappa > 0$ becomes

$$J = \begin{bmatrix} \omega' & -1 \\ 1 & 0 \end{bmatrix}, \tag{8}$$

where $\omega' = \omega/\kappa$. The eigenvalues are then given by

$$\lambda_{\pm} = \frac{\omega' \pm \sqrt{\omega'^2 - 2}}{2}. \tag{9}$$

One can show that the fixed point p_0 is a saddle point if and only if $|\omega'| > 2$. This condition depends only on ratio ω/κ. However, for the two other fixed points, the condition for them to be a saddle point depends on all parameters, κ, q, g and ω. As an example, one can show that the two fixed points are saddle points for $\kappa = 1$, $q = -0.6$, $g = 0.1$, and $\omega = 0.1$,

To compute the growth of the stable and unstable manifolds we use the search circle algorithm [11,12]. This algorithm is implemented in the dynamical system software (DSTOOL) [13].

Let us first look for some solutions of Eq. (1) with $\lim_{n\to\pm\infty} u_n = 0$. To find these solutions, we simply identify homoclinic points correspond to the fixed point p_0. That is, the intersection of the stable and unstable manifolds for the saddle point p_0. In Figure 2 we identify three homoclinic points: dot marker at (2.16,2.24), triangle marker at (-0.66,0.66) and square marker at (0.99,0.11). These homoclinic points leads to three different type of the solitons.

Let us choose for example the soliton obtained from the homoclinic point at (-0.66,0.66). We found that this type of soliton doesn't change much in the range $0 < \kappa < 1$. Figure 3 shows the soliton for $\kappa = 1$ and $\kappa = 0.005$.

Now, we will be interested in solitons with $\lim_{n\to\pm\infty} u_n = p_+$. We choose the parameters $\kappa = 1$, $q = -0.6$, $g = 0.1$ and $\omega = 0.1$. As stated before, the point p_+ is a saddle point. In Fig. 4 we identify three homoclinic points and their corresponding solitons. Next we plot the two manifolds for different values of the parameter κ. One can see from this figure that decreasing κ leads to disappearance of solitons. That is, we start with three homoclinic points and at $\kappa = 0.2$ we get two homoclinic points. By decreasing the value of κ, the two manifolds become tangent to each other and finally they will be separated, see Fig. 5.

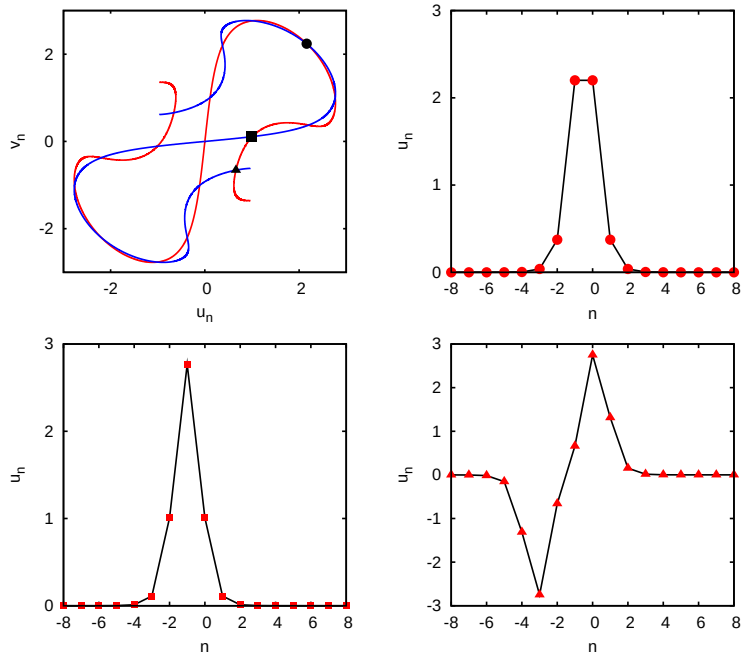

Figure 2. Type of solitons found from the homoclinic points. The stable (blue color) and unstable (red color) manifolds. There are three important homoclic points labeled by •, ▲ and ■. The parameters used are: $\kappa = 1$, $q = 1$, $g = 0.8$, $\omega = 10$.

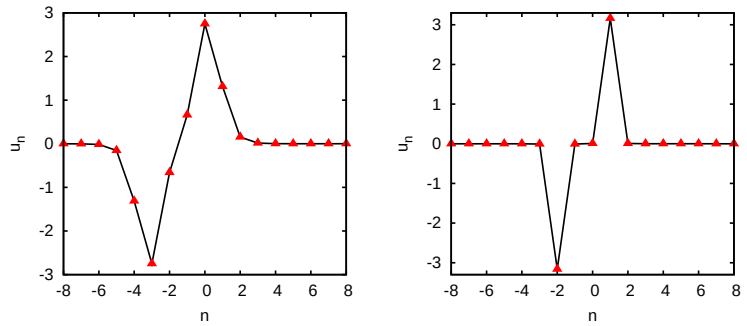

Figure 3. The parameters are $q = 1$, $g = 0.8$, $\omega = 10$ and different values of κ: (left) 1 and (right) 0.005.

In the next section, we study the linear stability of the solitons we found.

4. Stability analysis

Introducing a small perturbation to the solution of Eq. (1) as

$$\bar{\Phi}_n(t) = \left[u_n(t) + \epsilon\left(a_n \mathrm{e}^{-i\phi t} + b_n \mathrm{e}^{i\phi^* t}\right)\right] \mathrm{e}^{i\omega t}. \tag{10}$$

Inserting this last equation into Eq. (1), keeping linear terms with respect to ϵ, we obtain the equation of motion in the rotating frame as a set of linear differential equations

$$\dot{a}_n(t) = -\left(g u_{n-1} u_n + \kappa\right) a_{n-1} - \left(g u_{n-1}^2 + 2q u_n^2 + g u_{n+1}^2 - \omega\right) a_n - \left(g u_n u_{n+1} + \kappa\right) a_{n+1}$$

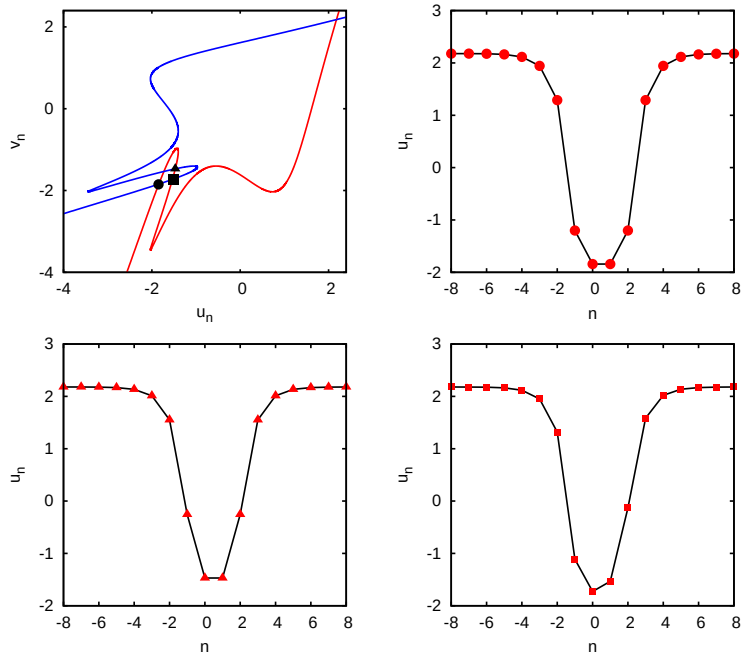

Figure 4. (left figure) Type of solitons found from the homoclinic points. (right figure) The stable (blue color) and unstable (red color) manifolds. Three important homoclic points labeled by •, ▲ and ■ are shown. The parameters used are $\kappa = 1$, $q = -0.6$, $g = 0.1$, $\omega = 0.1$.

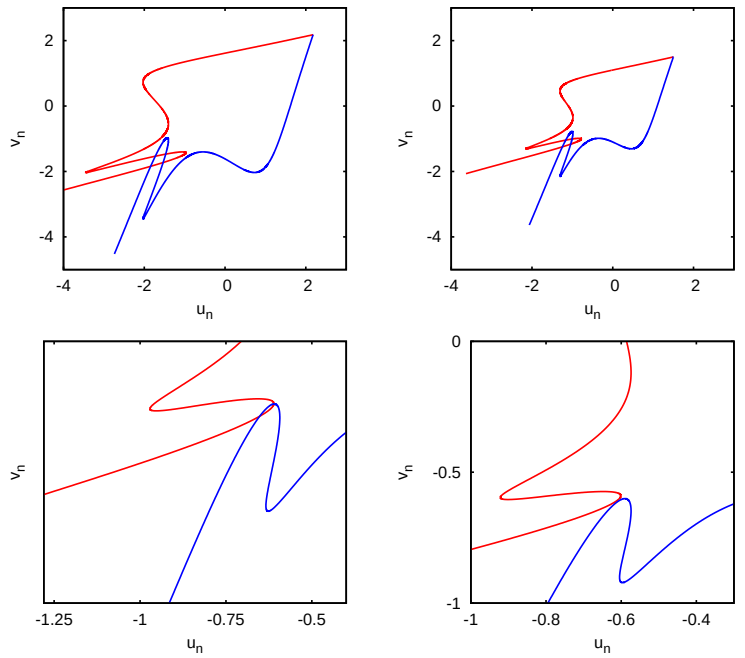

Figure 5. The stable (blue color) and unstable (red color) manifolds. The parameters used are $q = -0.6$, $g = 0.1$, $\omega = 0.1$ and different values of κ: $\{1, 0.5, 0.2, 0.19\}$.

$$-\left(gu_{n-1}u_n\right)b_{n-1} - \left(qu_n^2\right)b_n - \left(gu_nu_{n+1}\right)b_{n+1}, \tag{11}$$

$$\begin{aligned}\dot{b}_n(t) &= (gu_{n-1}u_n+\kappa)\,b_{n-1}+\left(gu_{n-1}^2+2qu_n^2+gu_{n+1}^2-\omega\right)b_n+(gu_nu_{n+1}+\kappa)\,b_{n+1}\\ &\quad+(gu_{n-1}u_n)\,a_{n-1}+\left(qu_n^2\right)a_n+(gu_nu_{n+1})\,a_{n+1}. \qquad (12)\end{aligned}$$

The eigenvalues of the linear system determine whether the solution is stable or not. Using Eq. (12) we found that in Fig. 2 symmetric odd mode (square marker) is stable however, the symmetric even mode (dot marker) is unstable. This is in accordance with [1]. In addition to that we found that the third soliton (triangle marker) is also stable. However, all the solutions in Fig. 4 are unstable.

5. Conclusion

The objective of this work was to obtain numerically the localized solutions of Eq. (1) using the homoclinic orbits method.The existence of the different type solutonic solutions have been shown and their linear stability have been checked.

Acknowledgments

This work has been supported by the research grant No. FRGS 0409-108 of the Ministry of Higher Education, Malaysia.

References

[1] Abdullaev F Kh, Baizakov B B, Darmanyan S A, Konotop V V, and Salerno M 2001 *Phys. Rev.* A **64** 043606
[2] Trombettoni A and Smerzi A 2001 *Phys. Rev. Lett.* **86** 2353
[3] Morsh O and Oberthaler M 2006 *Rev. Mod. Phys.* **78** 179
[4] Lahaye T, Menotti C, Santos L, Lewenstein M and Pfau 2009 *Rep. Prog. Phys.* **72** 126401
[5] Trefzger C, Menotti C, Capogrosso-Sansone B and Lewenstein M 2011 *J. Phys. B: At. Mol. Phys.* **44** 193001
[6] Fattori M, Roati G, Deissler B, D'Errico C, Zaccanti M, Jona-Lasinio M, Santos L, Inguscio M and G.Modugno 2008 *Phys. Rev. Lett.* **101** 190405
[7] Ai-Xia Zhang and Ju-Kui Xue 2010 *Phys. Rev.* A **82** 013606
[8] Rojas-Rojas S, Vicencio R A, Molina M I, and Abdullaev F Kh 2011 *Phys. Rev.* A **84** 033621
[9] Carretero-Gonzalez R, Talley J D, Chong C and B.A. Malomed 2006 *Physica* D **216** 77
[10] Carretero-Gonzalez R, Talley J D, Chong C and Malomed B A 2006 *Physica D* **216** 77
[11] England J, Krauskopf B and Osinga H M 2004 *SIAM Journal on Applied Dynamical Systems* **3** 161
[12] Krauskopf B and Osinga H M 1998 *J. Comput. Phys.* **146** 404
[13] DSTOOL Exploring dynamical systems, http://www.dynamicalsystems.org/sw/sw/